university of groningen

University Medical Center Groningen

University of Groningen

Weak ferromagnetism and exchange biasing in cobalt oxide nanoparticle systems

Tomou, A.; Gournis, D.; Panagiotopoulos, I.; Huang, Y.; Hadjipanayis, G. C. ; Kooi, B. J.

Published in:
Journal of Applied Physics

DOI:
10.1063/1.2207809

IMPORTANT NOTE: You are advised to consult the publisher's version (publisher's PDF) if you wish to cite from it. Please check the document version below.

Document Version
Publisher's PDF, also known as Version of record

Publication date:
2006

Link to publication in University of Groningen/UMCG research database

Citation for published version (APA):
Tomou, A., Gournis, D., Panagiotopoulos, I., Huang, Y., Hadjipanayis, G. C., & Kooi, B. J. (2006). Weak ferromagnetism and exchange biasing in cobalt oxide nanoparticle systems. *Journal of Applied Physics*, *99*(12), 123915-1 - 123915-5. [123915]. https://doi.org/10.1063/1.2207809

Copyright
Other than for strictly personal use, it is not permitted to download or to forward/distribute the text or part of it without the consent of the author(s) and/or copyright holder(s), unless the work is under an open content license (like Creative Commons).

The publication may also be distributed here under the terms of Article 25fa of the Dutch Copyright Act, indicated by the “Taverne” license. More information can be found on the University of Groningen website: https://www.rug.nl/library/open-access/self-archiving-pure/taverne-amendment.

Take-down policy
If you believe that this document breaches copyright please contact us providing details, and we will remove access to the work immediately and investigate your claim.

Downloaded from the University of Groningen/UMCG research database (Pure): http://www.rug.nl/research/portal. For technical reasons the number of authors shown on this cover page is limited to 10 maximum.

Download date: 05-05-2023

Weak ferromagnetism and exchange biasing in cobalt oxide nanoparticle systems

A. Tomou, D. Gournis, and I. Panagiotopoulos[a)]
Department of Materials Science and Engineering, University of Ioannina, Ioannina 45110, Greece

Y. Huang and G. C. Hadjipanayis
Department of Physics and Astronomy, University of Delaware, Newark, Delaware 19716

B. J. Kooi
Materials Science Centre, University of Groningen, Nijenborgh 4, 9747 AG Groningen, The Netherlands

(Received 2 February 2006; accepted 14 April 2006; published online 30 June 2006)

Cobalt oxide nanoparticle systems have been prepared by wet chemical processing involving the encapsulation of the nanoparticles by an organic ligand shell (oleic acid and oleylamine). CoO nanoparticles were easily prepared by this method, while the synthesis of the CoPt/CoO nanocomposites was achieved using a two step polyol process. CoPt nanoparticles were first obtained by simultaneous reduction of cobalt acetate and platinum acetylacetonate and then used as seeds for the growth upon them of cobalt oxide using a second polyol process. The antiferromagnetic CoO nanoparticles, when field cooled to temperatures below 200 K, show displacement of the magnetization curves (along the magnetization axis) characteristic of weak ferromagnetism phenomena that are attributed to the uncompensated surface magnetic moments. The transition temperature of the particles is considerably lower than the Néel temperature of CoO and it is followed by an upswing at low temperatures, which is attributed to spins that are loosely coupled to the antiferromagnetic core. In the CoPt/CoO nanocomposites, magnetic measurements show the appearance of increased coercivity with respect to the as-prepared CoPt particles and unidirectional anisotropy (loop shift of $H_{eb}=1125$ Oe) at temperatures below 20 K, as a result of exchange coupling between CoO and CoPt. © *2006 American Institute of Physics*.
[DOI: 10.1063/1.2207809]

I. INTRODUCTION

Weak ferromagnetism phenomena have been observed long ago in antiferromagnetic (AF) fine particles and have been explained as a result of unbalanced magnetic moments of the two magnetic sublattices due to their finite size.[1] The presence of uncompensated surface spins leads to anomalous magnetic properties, such as large moments, coercivities, and hysteresis loop shifts. In sufficiently small particles the reduced coordination of surface spins can cause a fundamental change in the magnetic order throughout the particle.[2] In this case a clear distinction between surface and bulk spin contributions to the total magnetic moment cannot be done. The development of modern deposition techniques permitted the extension of the studies in thin AF films. In particular, CoO (Refs. 3 and 4) has attracted a lot of interest due to its prototypical behavior as an antiferromagnetic oxide and its use in exchange biasing of ferromagnets (FMs) in AF/FM systems.

Exchange biasing is already in wide use in magnetoresistive read heads[5] and, furthermore, has been proposed as a means to stabilize the written information against thermal fluctuations in magnetic recording media.[6] Magnetic particles coupled to an antiferromagnetic substrate or matrix will increase its energy barrier due to the exchange coupling. Exchange biasing results when field cooling the sample through the Néel temperature (T_N) of the AF. The FM-AF interaction provides an effective bias field that gives rise to a horizontal shift of the hysteresis loop. The microscopic origin of exchange bias is still open to research due to the vast diversity of the systems in which it is observed and the lack of exact information on the surface spin structure. It is generally believed that the bias is related to defects in the antiferromagnetic order that lead to uncompensated spins inside the AF layers or at the AF interfaces.[7] More recent studies show that exchange biasing should be related to the "pinned" uncompensated interfacial spin, which do not rotate in an external magnetic field since they are tightly locked to the antiferromagnetic lattices.[8] Since these constitute only a small fraction (few percent) of a monolayer, this model can compromise the high unidirectional anisotropy values predicted by the model of Meiklejohn and Bean.[9] Therefore, it is of great interest to study these phenomena and their correlation.

In this work we report on the weak ferromagnetism phenomena in CoO nanoparticles and the exchange biasing of fcc-CoPt by cobalt oxide. CoO nanoparticles were prepared on the basis of a wet chemical processing involving the encapsulation of the nanoparticles by an organic ligand shell (oleic acid and oleylamine). The CoPt/CoO nanocomposites were synthesized by a two step polyol process with 1,2-dodecanediol as reducing reagent. Monodispersed CoPt nanoparticles were first obtained by simultaneous reduction of the corresponding precursors of the metal constituents.[10]

[a)]Electronic mail: ipanagio@cc.uoi.gr

 © 2006 American Institute of Physics

Downloaded 09 Feb 2007 to 129.125.25.39. Redistribution subject to AIP license or copyright, see http://jap.aip.org/jap/copyright.jsp

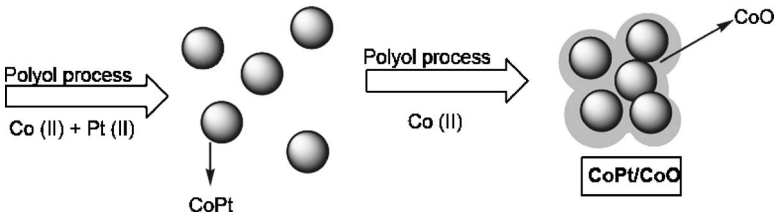

FIG. 1. Schematic representation of the overall synthetic process of CoPt/CoO nanocomposites.

Then a cobalt oxide shell was grown on the performed CoPt core based on a heterogeneous seeded growth reaction through another polyol process.

II. EXPERIMENTAL DETAILS

All chemicals were used as-received. Platinum acetylacetonate (97%), cobalt acetate (99.995%), diphenylether (99%), 1,2-dodecanediol (90%), oleylamine (70%, tech.), and oleic acid (90%, tech.) were supplied by Sigma-Aldrich. Absolute ethanol and acetone were obtained from Riedel-de Haën.

The polyol synthetic procedures were carried out in a spherical flask (50 ml) under reflux conditions and continuous stirring. CoO nanoparticles were prepared as follows: diphenylether (20 ml), 1,2-dodecanediol (1 mmol), and oleylamine (5 mmol) were mixed and the solution was heated at 140 °C for 10 min. Cobalt acetate (2.4 mmol) and oleic acid (5 mmol) were added afterwards to the solution and the temperature was raised to 180 °C. The reaction took place under these conditions for 3 h and the mixture was then cooled to room temperature. The CoO particles were precipitated with absolute ethanol (40 ml) and isolated by centrifugation. The precipitates were washed two times with ethanol and then centrifuged; the final CoO precipitate was dispersed with acetone and dried at room temperature.

The CoPt/CoO nanocomposites were prepared with a two step polyol process. In a typical experiment, the spherical flask was charged with diphenylether (20 ml), 1,2-dodecanediol (10 mmol), and oleylamine (5 mmol) and the solution was heated at 140 °C for 10 min. Platinum acetylacetonate (1 mmol), cobalt acetate (2.4 mmol), and oleic acid (5 mmol) were then added at the hot solution. The temperature was then raised to 185 °C and the reaction dwelled at these conditions for 3 h. Afterward the mixture was cooled at room temperature and the CoPt nanoparticles were precipitated with absolute ethanol (40 ml), isolated by centrifugation, washed, and centrifuged again.

The supernatant solution was discarded and the precipitates were added in the spherical flask with diphenylether (20 ml), 1,2-dodecanediol (1 mmol), and cobalt acetate (2.4 mmol). The solution was heated to 180 °C and the temperature was maintained for 1 h. The mixture was then cooled to room temperature and the CoPt/CoO nanocomposites were precipitated again with absolute ethanol (40 ml) and isolated by centrifugation. The precipitates were washed for another two times with ethanol and dried at room temperature.

The overall synthetic process of CoPt/CoO nanocomposites is schematically shown in Fig. 1.

In the first step Co (II) and Pt (II) cations are reduced to CoPt nanoparticles through the polyol process, while a second polyol step was used to grow a cobalt oxide shell upon the prepared CoPt nanoparticles.

X-ray powder diffraction data were collected on a D8 Advance Bruker diffractometer using Cu $K\alpha$ radiation and a secondary beam graphite monochromator. The patterns were recorded in the 2θ range from 2° to 100° in steps of 0.02 and counting time of 2 s per step. Magnetic measurements were carried out using a vibrating-sample magnetometer (VSM) (Lakeshore 3700) and a superconducting quantum interference device (SQUID) magnetometer (Quantum Design).

Transmission electron micrographs were obtained with JEOL 2010F and JEOL JEM-3010 microscopes equipped with energy dispersive x-ray analysis (EDAX) detectors. For the preparation of transmisston electron microscopy (TEM) samples a drop of the corresponding nanoparticle solution in hexane was deposited onto a holey-carbon grid and left to evaporate. The images are typical and representative of the samples under observation.

III. RESULTS ON CoO NANOPARTICLES

The x-ray diffraction (XRD) patterns of the CoO nanoparticles show only peaks of the cubic fcc cobalt monoxide structure (space group *Fm*-3*m*) with a lattice constant of 4.26 Å (Fig. 2). The peaks appear broadened due to the small size of the particles. An XRD estimation of the particle size can be done by the construction of the so-called Williamson-Hall plots[11] (Fig. 2, inset).

Figures 3(a) and 3(b) show typical high resolution TEM pictures of the 9 nm "XRD-size" nanoparticles. The (111) and (200) planes of the cubic CoO structure can be identi-

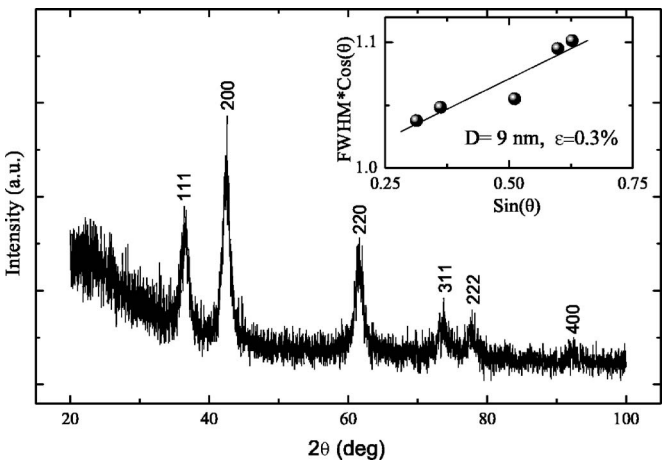

FIG. 2. XRD patterns of the CoO nanoparticles and Williamson-Hall plots of the FWHM cos θ vs sin θ (inset) used for an estimation of grain size.

Downloaded 09 Feb 2007 to 129.125.25.39. Redistribution subject to AIP license or copyright, see http://jap.aip.org/jap/copyright.jsp

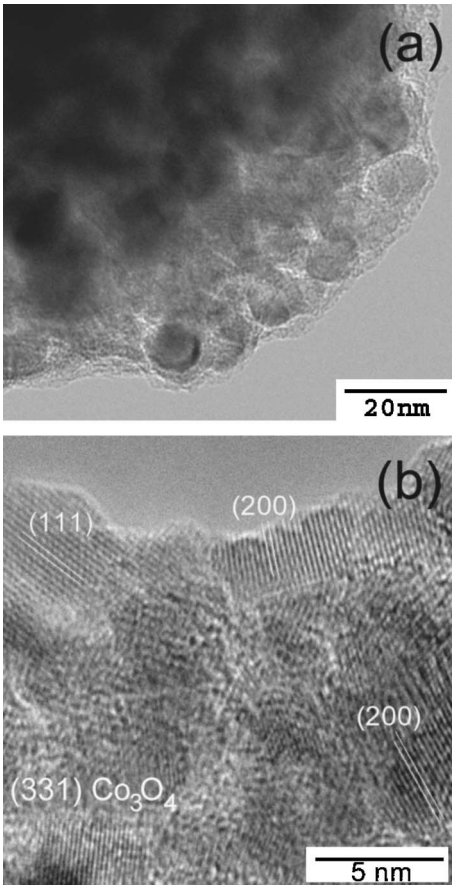

FIG. 3. High resolution TEM images of CoO nanoparticles.

fied. In some cases *d* spacings, which must be attributed to the (331) planes of the Co_3O_4 cubic spinel structure with $a = 8.09$ Å, are identified. These reflections do not appear in the XRD patterns probably due to the small percentage and the nanocrystallinity of the phase. Despite the large particle overlap, it seems that the particles have spherical-like shapes without any specific faceted structures. The tendency of a nanoparticle to assume specific faceted structures would be of great importance to the total uncompensated moment observed since it depends on both the crystallographic direction of the surface and its roughness.[7]

The above sample shows some typical "weak-ferromagnetic" features originating from the uncompensated moments that are overlayed on the typical linear AF response. The loop measured at 5 K after field cooling under 50 kOe (inset Fig. 4) appears displaced along the magnetization axis, which indicates that after the field cooling process there is a fraction of the pinned uncompensated moments that are characterized by very high local anisotropy field values and cannot be rotated under the maximum field used. The rotatable magnetic moments show a small hysteresis of 900 Oe. Assuming 9 nm particles the offset amount of 0.85 emu/g corresponds to a 2% fraction of pinned uncompensated surface moments.

In order to probe the temperature dependence of the pinned moments, we have measured the temperature dependence of the remanent magnetization. The measurements were taken under a field of 1 kOe during warm up after field cooling under 50 kOe. The resulting thermoremanent curve (TMR, Fig. 4) shows a broad transition around 200 K, which is lower than the T_N of the bulk CoO AF phase of 290 K by 30%. The transition is followed by an upturn of the thermomagnetic curve below 15 K. This upturn could be attributed to the presence of a Co_3O_4 secondary phase. The bulk critical temperature of Co_3O_4 is 40 K, which would imply a 60% decrease due to size or superparamagnetic effects. This possibility cannot be excluded; however, the shape of the curve and the characteristic temperatures are similar to the ones that have been observed in thin AF CoO layers of the order of 2 nm (Ref. 4) and are attributed to a fraction of spins which are more loosely coupled.[7]

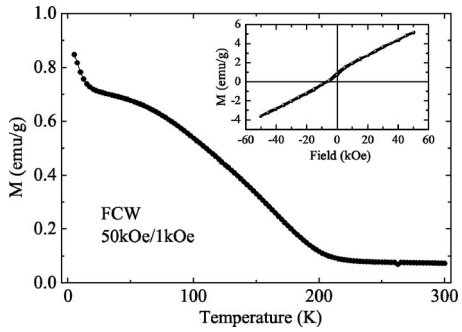

FIG. 4. Thermoremanent magnetization measured under a field of 1 kOe during warm up after field cooling under 50 kOe. Inset: Hysteresis loop monitored at 5 K after field cooling under 50 kOe.

IV. RESULTS ON CoPt/CoO NANOCOMPOSITES

CoPt nanoparticles prepared by the chemical synthesis route have been used as seeds for the preparation of CoPt/CoO nanocomposites as described above.

In Fig. 5 the XRD diffraction patterns of the as-prepared CoPt sample and the CoPt/CoO are compared. Only the peaks of the disordered fcc-CoPt structure are clearly observed. The width of the peaks indicates a size of 4 nm. This is in fair agreement with the TEM pictures in which the *d* spacings of the fcc-CoPt structure can be seen [Figs. 6(a) and 6(b)]. The CoO shell is not easily discerned, probably due to its small thickness and amorphicity and particle overlapping. Strangely, in several cases, a *d* spacing of 1.7 Å is observed, which coincides with the (201) reflection of the ordered tetragonal structure $L1_0$. Furthermore, in few cases, *d* spacings that can be attributed to the Co_3O_4 spinel structure have been

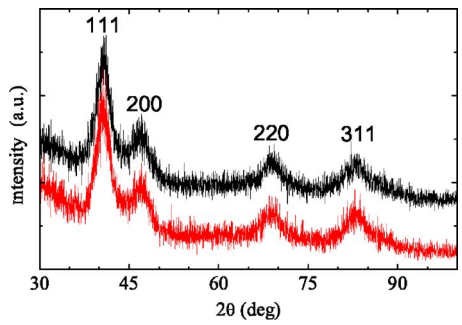

FIG. 5. (Color online) X-ray diffraction patterns of the as-prepared CoPt sample (top) and the CoPt/CoO nanocomposite (bottom).

Downloaded 09 Feb 2007 to 129.125.25.39. Redistribution subject to AIP license or copyright, see http://jap.aip.org/jap/copyright.jsp

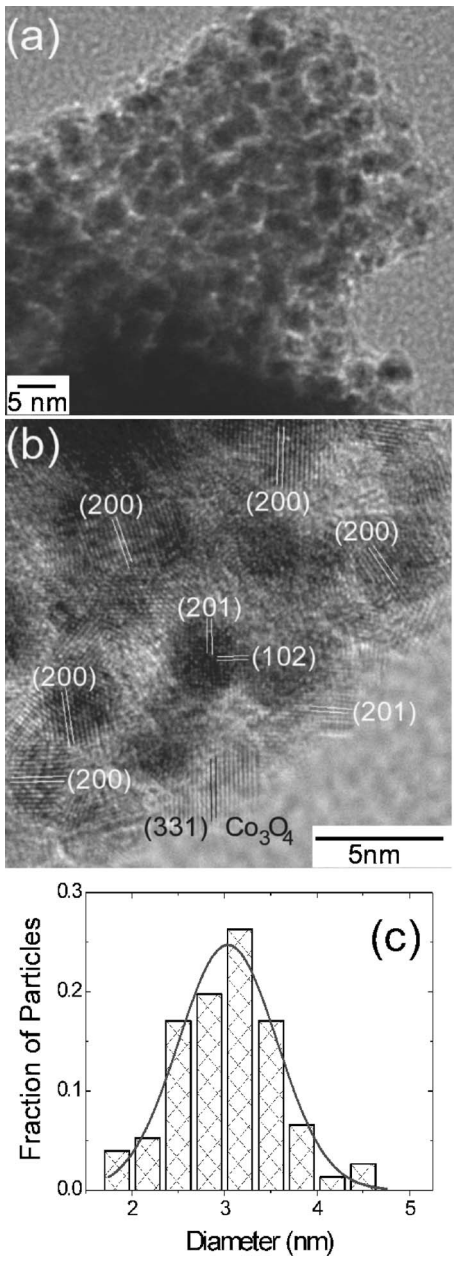

FIG. 6. High resolution TEM images of CoPt/CoO nanocomposite. The (*hkl*) of the CoPt phase are indicated with white letters. Lower panel: Particle size distribution. The continuous line represents a Gaussian fit.

observed as the one shown in Fig. 6(b). These are not observed in the XRD patterns. By measuring the sizes of 76 different particles from different TEM images we get the size distribution presented in Fig. 6(c). The mean size can be estimated to 3 nm with the standard deviation of 0.6 nm. As far as the magnetic response is concerned, the mean size related must be weighted by D^3, which leads to a slightly higher mean value of 3.3 nm. Before discussing the exchange phenomena observed in the nanocomposites we briefly present the magnetic hysteresis of as-prepared fcc-CoPt nanoparticles to serve as a basis for comparison. The hysteresis loops measured at low temperatures are presented in Fig. 7. The low coercivities and the steep high field slopes (χ_{HF}) of the magnetization curves indicate that the size of the nanoparticles is in the limit of the superparamagnetic behavior. Indeed considering the low anisotropy of the disordered fcc-CoPt phase ($K=8\times10^5$ erg/cm^3),[12] the expected critical size for a blocking temperature (T_B) of 5 K is only 3.5 nm and for T_B of 10 K, only 4.3 nm. Therefore a large fraction of the nanoparticles will be superparamagnetic even at low temperatures. This is further supported by the rapid loss of remanence with temperature and the fact that χ_{HF} seems to scale with temperature as $1/T$ above 10 K (inset of Fig. 7).

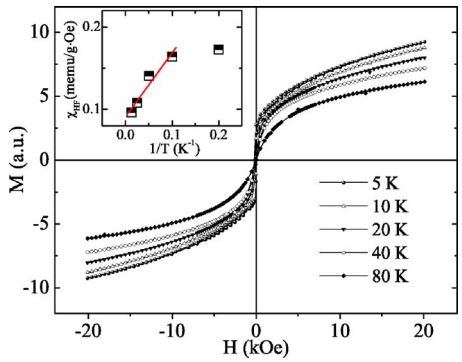

FIG. 7. (Color online) Hysteresis loops of the as-prepared CoPt measured at low temperatures (5–80 K as indicated). Inset: Temperature dependence of the high field slope.

When these particles are used as seeds for the growth of oxide layers, the appearance of exchange anisotropy is expected. Indeed when field cooled (FC) the hysteresis loops of the CoPt/CoO nanocomposites appear displaced with respect to the field axis, indicating the presence of unidirectional anisotropy (Fig. 8). In this case the exchange bias field H_{eb} can be defined as the amount of loop displacement and the coercivity H_C as the half-width of the loop. The temperature variation of H_{eb} and H_C are given in Fig. 9 and are compared with the H_C of the symmetric zero-field-cooled (ZFC) loop of CoPt/CoO as well as with the H_C of CoPt. In an exchange biased system loop displacement can be observed in the limit where the coupling energy per unit area J between the ferromagnetic and the antiferromagnetic phases is weak compared to the anisotropy energy of the AF layer. This is expressed by the relation $J<K_{AF}\cdot t_{AF}$, with t_{AF} the thickness and K_{AF} the anisotropy of the AF layer.[13] Otherwise, the FM and AF spins rotate simultaneously, resulting in an increase of the coercivity. In our case the increase in H_C is more pronounced than the H_{eb} itself, indicating that we are in the limit of strong coupling, probably due to the thin AF layer thickness.

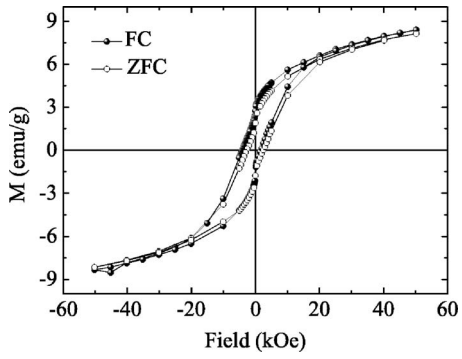

FIG. 8. Hysteresis loops of the CoPt/CoO nanocomposite measured at 5 K after field cooling in 50 kOe (FC) or zero field cooling (ZFC).

Downloaded 09 Feb 2007 to 129.125.25.39. Redistribution subject to AIP license or copyright, see http://jap.aip.org/jap/copyright.jsp

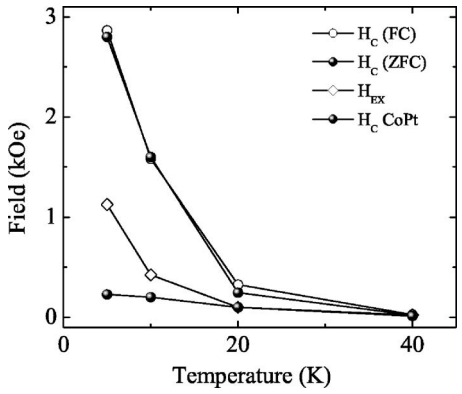

FIG. 9. Temperature dependence of H_C(FC), H_{ex}(FC), and H_C(ZFC) of CoPt/CoO compared to the H_C of the CoPt nanoparticles.

This may also explain the relatively low interface energy value that can be calculated, assuming 3.3 nm spherical particles and the bulk saturation magnetization value for the core FM phase,[13] as $J=M_S H_{eb} D/6=0.05$ erg/cm^2.[14] Indeed this value is on the low side compared to the values of 0.03–3.5 erg/cm^2 typically observed in CoO exchange biasing systems,[13] the highest of which has been obtained in oxidized Co particles. However, this is just an "effective" J in which the fraction of the strongly coupled spins is not taken into account. The observed values of coercivity and blocking temperature are consistent with a 3.3 nm size and effective anisotropy constant of 2.6×10^6 erg/cm^3. If we assume that the core retains its bulk anisotropy value of $K_V = 8\times10^5$ erg/cm^3, then interfacial anisotropy due to the presence of the oxide layer must be of the order of $K_S = 0.1$ erg/cm^2 according to

$$K_{\text{eff}} = K_V + \frac{6}{D}K_S \tag{1}$$

that holds for a spherical particle of diameter D. The low blocking temperature of the exchange anisotropy effects must be attributed to the small thickness of the oxide layers.

V. SUMMARY AND CONCLUSIONS

Cobalt oxide nanoparticles have been prepared by a standard polyol-synthesis process. When field cooled to temperatures below 200 K, the nanoparticles show a small hysteresis and displacement of the magnetization curves (along the magnetization axis) characteristic of weak ferromagnetism phenomenon, accompanied by high magnetic anisotropy. The transition temperature of the particles is considerably lower than the Néel temperature of CoO and it is followed by an upswing at low temperatures, which is attributed to spins that are loosely coupled. The same chemical synthesis method has been applied in two steps in order to modify the surface of fcc-CoPt nanoparticles that have been used as seeds. The surface modification leads to the appearance of exchange anisotropy and a substantial increase of the coercivity. This shows that the interfacial coupling J is too strong to satisfy the condition $J < K_{AF}\cdot t_{AF}$ for exchange anisotropy. If instead we are in the limit of strong coupling, the FM and AF spins rotate simultaneously, resulting in an increase of the coercivity.

[1] See, for instance, A. H. Morrish, *The Physical Principles of Magnetism* (Wiley, New York, 1965).
[2] H. Ohldag, A. Scholl, F. Nolting, E. Arenholz, S. Maat, A. T. Young, M. Carey, and J. Stohr, Phys. Rev. Lett. **91**, 017203 (2003).
[3] T. Ambrose and C. L. Chien, Phys. Rev. Lett. **76**, 1743 (1996).
[4] Y. J. Tang, D. J. Smith, B. L. Zink, F. Hellman, and A. E. Berkowitz, Phys. Rev. B **67**, 054408 (2003).
[5] B. Dieny, V. S. Speriosu, S. Metin, S. S. P. Parkin, B. A. Gurney, and P. Baumgart, J. Appl. Phys. **69**, 4774 (1991).
[6] V. Skumryev, S. Stoyanov, Y. Zhang, G. Hadjipanayis, D. Givord, and J. Nogues, Nature (London) **423**, 850 (2003).
[7] K. Takano, R. H. Kodama, A. E. Berkowitz, W. Cao, and G. Thomas, Phys. Rev. Lett. **79**, 1130 (1997).
[8] R. H. Kodama, S. A. Makhlouf, A. E. Berkowitz, Phys. Rev. Lett. **79**, 1393 (1997).
[9] W. H. Meiklejohn and C. P. Bean, Phys. Rev. **102**, 1413 (1956).
[10] S. Sun, C. B. Murray, D. Weller, L. Folks, and A. Moser, Science **287**, 1989 (2000).
[11] G. K. Williamson and W. H. Hall, Acta Metall. **1**, 22 (1953).
[12] R. A. McCurrie and P. Gaunt, Philos. Mag. **13**, 567 (1966).
[13] J. Nogues and I. K. Shuller, J. Magn. Magn. Mater. **192**, 203 (1999).
[14] U. Wiedwald, J. Lindner, M. Spasova, Z. Frait, and M. Farle, Phase Transitions **78**, 85 (2005).

Downloaded 09 Feb 2007 to 129.125.25.39. Redistribution subject to AIP license or copyright, see http://jap.aip.org/jap/copyright.jsp